

## Laser-launched flyer plates for shock physics experiments

Damian C. Swift,<sup>a)</sup> Johnathan G. Niemczura,<sup>b)</sup> Dennis L. Paisley, Randall P. Johnson, Sheng-Nian Luo, and Thomas E. Tierney IV

*P-24 Plasma Physics, Los Alamos National Laboratory, MS E526, Los Alamos, New Mexico 87545*

(Received 15 October 2004; accepted 13 August 2005; published online 19 September 2005)

The TRIDENT laser was used to launch Cu, Ga, and NiTi flyers from poly(methylmethacrylate) (PMMA) substrates, coated with thin ( $\sim$ micron) layers to absorb the laser energy, confine the plasma, and insulate the flyer. The laser pulse was  $\sim$ 600 ns long, and the flyers were 50 to 250  $\mu$ m thick and 4 mm in diameter. With an energy of 10–20 J, speeds of several hundred meters per second were obtained. Simulations were performed of the flyer launch process, using different models. The simulations reproduced the magnitude of the flyer speed and qualitative variations with drive energy and design parameters, but systematically overpredicted the flyer speed. The most likely explanation is that some of the laser energy was deposited in the transparent substrate, reducing the amount available for acceleration. The deceleration of the flyer was measured on impact with a PMMA window. Given the equation of state and optical properties of PMMA, the deceleration allowed points to be deduced on the principal Hugoniot of Cu. The points deduced were in good agreement with the published equation of state for Cu, suggesting that there was no significant preheating of the flyer or other systematic effects which might reduce the accuracy of equation of state measurements. © 2005 American Institute of Physics. [DOI: 10.1063/1.2052593]

### I. INTRODUCTION

Laser-launched flyers offer great promise for shock physics experiments, for investigating the dynamic properties of materials such as the equation of state (EOS), strength, and phase changes. The flyer—typically a thin disk launched from a transparent substrate—is accelerated by directing a laser pulse through the substrate to vaporize a layer of material, which then exerts pressure on the flyer. Shock physics experiments are performed by allowing the flyer to impact a stationary target, and measuring properties of the shocked state. Laser launching has advantages compared with older techniques such as propellant or gas guns and chemical explosives<sup>1</sup> because there is relatively little momentum or energy associated with the acceleration process, so the apparatus can be significantly smaller and recovery of the sample significantly easier. This lack of collateral damage also reduces the cost per shot. The time over which acceleration occurs is much shorter than in a gun, so it is easier to synchronize diagnostics with the shock event. A relatively high shot rate can be maintained—we have routinely achieved 10–15 high-quality experiments per day, compared with one or fewer on a gun—which, together with the lower cost, makes it possible to address one of the chronic problems of shock experiments, which is a paucity of repeat experiments and poorer statistics than in most other fields of physics. It also opens the possibility of exploring systematic effects which would not otherwise be practicable, such as the response of samples of many different combinations of crystal orientation: a key requirement in testing microstructurally based theories of material response. Laser

flyer experiments make it convenient to study small samples, a significant benefit when dealing with toxic, radioactive, or expensive materials.

There are potential drawbacks in laser launching of flyers. The temperature in the plasma may reach thousands of Kelvin. A commonly raised concern is that heat may be transferred to the bulk of the flyer, altering the state induced in the target on impact and reducing the accuracy of shock measurements. *In situ* temperature measurements of the flyer are difficult, particularly when spectral channels for pyrometry must be shielded carefully from stray laser light. An alternative way to investigate the accuracy is to perform measurements on well characterized materials, testing whether laser flyers can reproduce results obtained from alternative experimental techniques.

We have developed laser flyers for shock physics experiments, building on technology intended originally for laser initiation of chemical explosives,<sup>2–4</sup> but scaled up to allow experiments to be performed in conditions similar to those accessible with a gas gun. Flyer acceleration histories were obtained by Doppler velocimetry for a range of laser and flyer parameters, including the flyer material (Cu or NiTi). Simulation techniques were investigated to explore the physical processes involved in flyer launch, and to allow the launch system to be optimized for different applications. Impact experiments were performed with Cu flyers, to test the accuracy with which a known EOS could be reproduced. Experiments were also performed with Ga flyers, as a sensitive demonstration that preheating of the flyer is negligible.

Since the concept of launching flyers from a transparent substrate was first reported, other researchers have developed and reported similar systems and their applications to shock physics experiments, typically with a laser pulse around 10 ns long delivering up to 1 J.<sup>5–7</sup> The novelty of the work

<sup>a)</sup>Electronic mail: dswift@lanl.gov

<sup>b)</sup>Present address: The University of Texas, Austin.

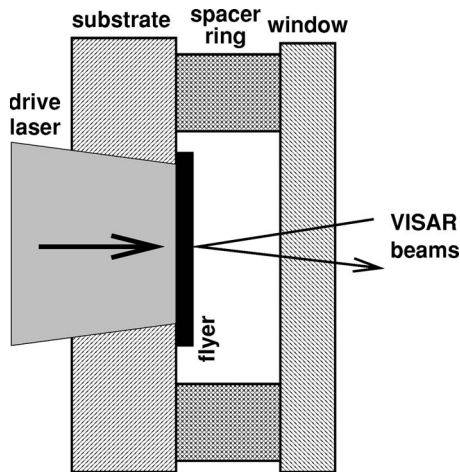


FIG. 1. Schematic of flyer impact experiments.

presented here is in the use of much longer laser pulses, allowing flyers to be launched which are thick enough to permit meaningful comparison with data from gun-launched flyers, and also the inclusion of simulations of the launch process. Flyers have also been launched by unconfined laser ablation,<sup>8–10</sup> which is a qualitatively different process of much lower efficiency;<sup>11</sup> it has been considered as a method of launching satellites.<sup>11</sup>

## II. LASER-DRIVEN FLYER PLATES

The flyer on its substrate was spaced off from an impact window. The substrate and impact window were both planar disks of poly(methylmethacrylate) (PMMA). The complete assembly was screwed together in a reusable target holder. Experiments were performed in vacuum at the TRIDENT laser facility at Los Alamos (Fig. 1).

### A. Flyer assembly

The flyer assembly comprised a disk-shaped flyer 4–6 mm in diameter and with a variety of thicknesses from 50 to 250  $\mu\text{m}$ , attached to a PMMA substrate 3 mm thick, which had been coated with layers of carbon, alumina, and Al (Fig. 2). The carbon was intended to absorb the laser energy and form a vapor or plasma which would act as the working fluid to accelerate the flyer; the alumina and Al were intended to

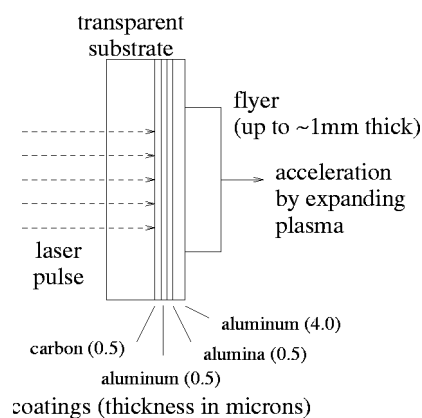


FIG. 2. Detail of coatings between substrate and flyer.

insulate the flyer from conducted heat and to prevent the working fluid from expanding sideways.<sup>2–4</sup> In some cases the flyer disk was deliberately wider than the laser spot: the laser drove a “bubble” of the disk outward to form the flyer; while the edges remained in contact with the substrate, preventing the working fluid from escaping radially.

Cu foils were purchased from Goodfellow Corp; flyers were punched from this stock. The foils had distinct striations and machining marks. We attempted to remove these from the surface to avoid the generation of interference patterns which might interfere with the laser velocimetry measurements, by polishing the surface manually using diamond paste. This was only partially successful. Flyers were also made from Ga, cast into disks of 6 mm diameter and 50–100  $\mu\text{m}$  thick, and also NiTi alloy, cut from a cast rod, ground to 50–200  $\mu\text{m}$  and polished.

Each flyer was attached to its substrate with five-minute epoxy glue. A bubble-free drop, around 5 mm<sup>3</sup> in volume, of freshly mixed glue was placed at the center of the coated face of the substrate. The flyer was pushed gently into the glue, then clamped in place between parallel, circular faces, with a pressure of around 0.5 MPa until the glue had set. The pressure of the clamp squeezed the excess glue—almost all of it—radially outward. The viscosity of the glue was sufficiently low, and the time before the glue set was sufficiently long, that the thickness of glue remaining should be negligible compared with the surface finish of the coating and the flyer. A conservative estimate of the maximum thickness of any glue present is thus 2  $\mu\text{m}$ .

### B. Drive beam

The drive pulse was generated by one of the main TRIDENT beams. TRIDENT is based around a Nd:glass laser with a fundamental wavelength of 1054 nm. A key aspect of laser launching of flyers is that the pressure pulse and, hence, the laser pulse should be chosen for reasonably optimal coupling to the flyer. Under normal operating conditions, the pressure in the working fluid rises with energy deposited, and is relieved as the flyer accelerates and the substrate recoils. The rising pressure in the working fluid drives a compression wave into the flyer, and back into the substrate. In most materials, the sound speed increases with pressure, so the compression wave steepens as it propagates, and may ultimately become a shock wave. Thus, if the pulse intensity rises too quickly, a shock wave would be induced in the flyer, causing irreversible heating. The maximum rate of increase that can be tolerated depends on the peak pressure and the flyer thickness, but should be of similar order to the transit time of sound through the flyer. If the pulse duration is shorter than the time for the compression wave to travel through the flyer and for release from the free surface of the flyer to then travel back to the working fluid, interactions between the release waves from the drive and free surfaces may interact, inducing tension which may damage and spall the flyer. If the drive pressure is comparable with the flow stress of the flyer material, strong elastic oscillations may be set-up in the flyer. Conversely, if the pulse is long enough for conduction to be significant, the flyer may be heated by the working fluid. Another constraint on the pulse length is that

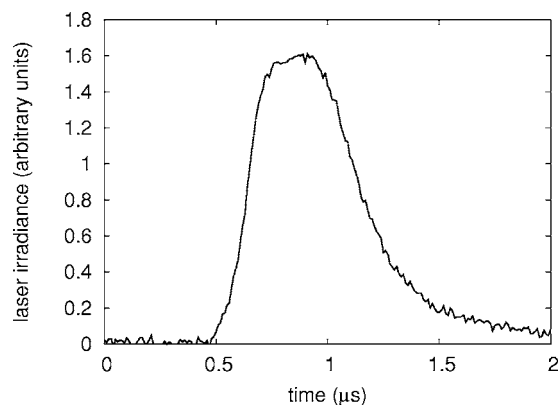


FIG. 3. Example temporal history of laser pulse. The pulse shape was reproducible.

if the flyer accelerates over a distance significant compared with the diameter, it may become appreciably curved, reducing its suitability for shock impact experiments which are ideally one-dimensional. For the flyers used here, the laser pulse should be several hundred nanoseconds long.

The laser was operated in long-pulse mode, using a pulse-stretching technique. Frustrated amplification was used to stretch the pulse: an arbitrary wave form generator was used to drive an acousto-optical modulator positioned within the laser; the laser pulse was permitted to buildup for a short time, then the transmission of the crystal was reduced to reduce the amplification rate. The pulse shape produced by the wave form generator was altered until the laser pulse lasted the desired duration. The drive pulse was chosen to be  $\sim 600$  ns long (full width at half maximum). The pulses generated were asymmetric in time, with a long tail. The drive energy was measured with a calorimeter, and the irradiance history of the drive pulse with a photodiode. The uncertainty in energy was of the order of 1 J at most. The pulse shape was reasonably repeatable at all energies used (Fig. 3).

A random-phase plate (RPP) was used to smooth the beam; this made a significant improvement to the spatial uniformity. The beam optics were arranged to give a spot  $\sim 4$  mm in diameter on the substrate. The beam irradiance was well below the threshold to cause damage to the RPP. Except at the lowest energies, the compression wave from the working fluid induced spall and fragmentation of the free surface of the substrate; fragment impact was the principal potential source of damage to the RPP. Although debris did impact the RPP, initial trials with a fragment shield showed that no significant damage was caused by the debris, so the RPP shield was omitted in subsequent experiments. The surface of the RPP became misty after a couple of shots; this did not degrade the energy imparted to the flyer to any appreciable extent, and no larger-scale damage was observed after repeated firings through the same region of the RPP (as was feared if the misty layer absorbed much of the laser energy). We moved the RPP to expose a fresh region once during this series of experiments. The cause of the misting was not determined; one possibility was thought to be the oxidation of a layer of grease collected during storage. However, a surface previously cleaned with ethanol also became misty.

The nominal (requested) laser energy was 5, 10, or 20 J;

the energy delivered was usually within 1 J of the request. TRIDENT was capable of delivering up to 400 J at this wavelength, but damage was caused to the RPP at energies over 35 J.

### C. Diagnostics

The velocity history of the flyer was measured by time-resolved laser Doppler velocimetry, measured by interferometry of the VISAR type.<sup>12</sup> A line-imaging VISAR was used on all experiments, and a point VISAR on some.

Line VISAR illumination was provided by a pulsed Nd:yttrium-aluminum-garnet laser, operating at 1319 nm wavelength and frequency doubled to 660 nm. The laser pulse was stretched to about  $1.5 \mu\text{s}$  to capture the acceleration and impact of the flyer, again using an acousto-optical modulator as for the drive pulse. A continuous wave laser of 532 nm was used for the point VISAR. Line VISAR fringes were recorded using an optical streak camera. Timing markers were incorporated on the streak record, at intervals of 200 ns. The fringe constant of the VISAR was computed from the thickness of the delay element (9.970 in. of BK7 glass). The dispersion of the glass was determined at the wavelength of the probe laser by fitting a straight line to points sampling the variation of refractive index with wavelength. The fringe constant deduced was 216 m/s at 660 nm. The relative timing of the point and line VISARs was deduced by comparing the position at which a shock wave appeared in a flyer impact experiment. The relative timing had an uncertainty of around 3 ns.

The line-imaging VISAR was used to measure the flatness of the flyer; the point VISAR provided a more accurate velocity averaged over a small region. The velocities from both VISARs were consistent. The flyer decelerated on impact with the window: this provided a direct measure of flatness after several hundred microns of flight. The deceleration also provided the raw observable for determining shock states and, hence, measurements of the EOS. A distance-time record was inferred by integrating each velocity history.

Because of noise in the signals, the acceleration histories exhibited some undulations caused by difficulties in locating the zero in the phasor diagram. There was no absolute time reference between the drive pulse and the acceleration history.

### III. ACCELERATION PERFORMANCE

We have performed many tens of experiments with the flyer assembly as described earlier, and also with variants such as different substrates and working fluids. The series of experiments with PMMA coated as above are the best starting point for studies of the launch process, as some experiments were intended specifically for measurements of the acceleration history. No target was included other than a transparent window, allowing the full diameter of the flyer to be observed. Here we consider experiments performed principally with Cu flyers, but also including some made from NiTi and Ga. Different materials allow the variation of mass density to be studied: this would be expected to affect the

TABLE I. Acceleration experiments with Cu flyers.

| Shot   | Flyer thickness ( $\mu\text{m}$ ) | Drive energy (J) | Residual pressure (MPa) |
|--------|-----------------------------------|------------------|-------------------------|
| 14 119 | 105                               | 10               | 10                      |
| 14 120 | 105                               | 5                | 0                       |
| 14 121 | 105                               | 20               | 20                      |
| 14 129 | 55                                | 11               | 10                      |
| 14 130 | 55                                | 19               | 10                      |
| 14 131 | 55                                | 5                | 10                      |
| 14 132 | 250                               | 11               | 40                      |
| 14 134 | 250                               | 24               | 60                      |
| 14 135 | 250                               | 5                | 70                      |

recoil of the substrate. Experiments also explored the effect of different flyer thickness and drive energy (Table I).

The acceleration correlated with the irradiance of the drive pulse, with some further acceleration ( $\sim 10\%$  in speed) after the end of the pulse caused by expansion of the plasma. Most of the flyers were still accelerating slightly at the end of the record. There was evidence of ringing during acceleration, but no sign of shock formation or spall in the flyers. The  $250\ \mu\text{m}$  Cu flyers appeared to show an increased acceleration after the drive pulse compared with the thinner flyers; the time scale was too long to correspond with reverberations in the plate. One cause might be a radial reflection in the plasma after it had expanded to the sides of the target holder. The velocity ranges covered by varying the drive energy and flyer thickness were large enough to give an overlap between each group. The displacement history was used to predict the impact time with a stationary window: this provided a sensitive check on the velocity (Figs. 4 and 5).

Apart from a slight lag at the edges, all the flyers were flat to within the accuracy of the data (Fig. 6). In most cases, the accuracy was dominated by the uncertainty in spatial wavelength of the fringes. If the line VISAR record comprised many closely spaced fringes then the uncertainty in the initial position of each fringe—and hence, in the wavelength—was quite large.

The speed of the flyer increased monotonically with la-

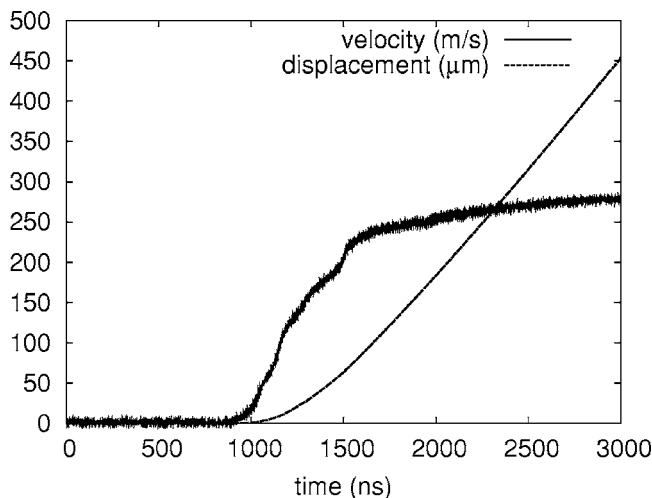


FIG. 4. Example of acceleration and displacement history (shot 14 119:  $105\ \mu\text{m}$  Cu flyer, 10 J drive).

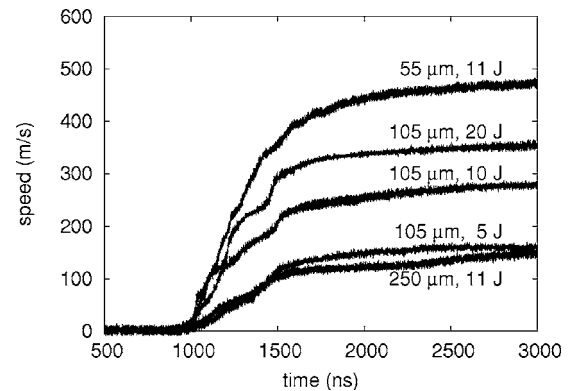


FIG. 5. Velocity history for Cu flyers.

ser energy, and decreased monotonically with flyer thickness (Fig. 7). Comparing the laser energy delivered per flyer mass with the specific kinetic energy of the flyer, an approximately linear relation was observed for each flyer thickness, indicating a constant efficiency of energy conversion across each group. The efficiency ranged from  $\sim 1\%$  for  $250\ \mu\text{m}$  Cu flyers to  $\sim 3\%$  for  $55\ \mu\text{m}$  Cu flyers. This variation probably reflects the increased energy imparted to the substrate with thicker flyers. Comparing Cu with NiTi, the terminal velocity correlated with areal mass: Cu at  $100\ \mu\text{m}$  thick was similar to NiTi at  $150\ \mu\text{m}$  thick; thicknesses matching the relative density (Fig. 7).

The relatively small acceleration present at the end of each record was used to estimate a residual pressure behind the flyer, by dividing the acceleration by the areal mass of the flyer. The acceleration was estimated by fitting a straight line to the last section of each record. In all cases, the residual pressure was small compared with typical impact pressures generated by flyers at these speeds and compared with typical spall strengths, so the presence of residual plasma at this pressure would not be expected to perturb materials experiments (Table I).

In the experiments with a Ga flyer, the surface reflectivity was high and uniform throughout the acceleration process. This suggests that the front surface of the flyer was no hotter than the melting temperature of Ga:  $29.8\ ^\circ\text{C}$ .

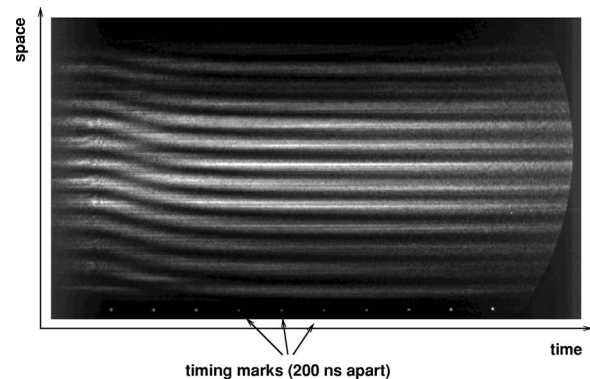


FIG. 6. Line VISAR record for shot 14 119. Fringes are displaced spatially as the flyer accelerates: the displacement is proportional to the speed. The field of view was 4 mm, centered on the center of the flyer. The flyer diameter was 5 mm.

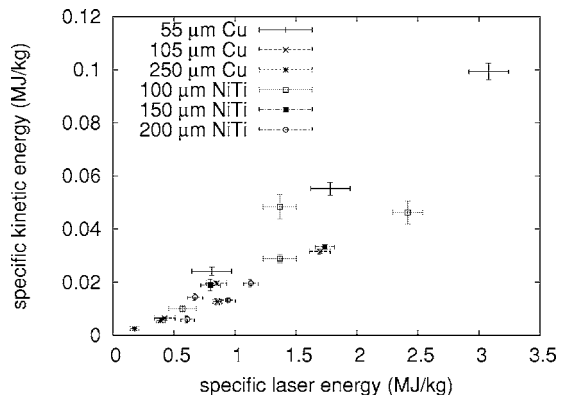


FIG. 7. Variation of flyer kinetic energy with specific laser energy measured against flyer mass.

#### IV. SIMULATION OF FLYER ACCELERATION

A calculational study was performed to investigate whether the velocities obtained were reasonable, and in particular that the nominal efficiency of converting laser to kinetic energy suggested that all the energy was deposited in the working fluid. If the efficiency predicted using this assumption was much higher than observed, it would be an indication that fast electrons or x rays could be produced (possibly heating the flyer or target), that the laser energy may be absorbed in the transparent substrate (limiting the possibilities of increasing the flyer speed by supplying more energy), or that heating of the working fluid may be limited by laser-plasma instabilities such as stimulated Raman or Brillouin scattering (again limiting the value of supplying more drive energy, and also risking damage to the drive laser). A calculational capability also allows the design parameters to be optimized to increase the efficiency.

Laser energy is deposited in the working fluid; if the final temperature of the fluid is very high, it might constitute a significant fraction of the drive energy. If the layer is thick or of high density, its kinetic energy could be considerable. If the density of the substrate is low or its compressibility high, its recoil would reduce the energy transferred to the flyer; thicker substrates are preferable in this respect. If the working fluid escapes laterally from behind the flyer—as should happen once the flyer has traveled far enough for the confining layers to rupture—then the pressure accelerating the flyer would fall to zero. A fraction of the laser energy fails to reach the working fluid, because of reflection from surfaces encountered on the way (including the free surface of the substrate) or if it is absorbed in the bulk of the substrate. Absorption in the substrate may change during the drive pulse, as the compression wave traveling through the substrate may alter its optical properties—particularly once the wave reaches the free surface. The substrate may also accumulate damage from deposited energy. Substrates recovered from these experiments were damaged at the free surface, often by cratering as could be caused by spall induced by the compression wave. At higher energies, material at the surface of the crater was brown or black, suggesting that a significant amount of laser energy was deposited there. Energy is lost from the working fluid by radiation through the substrate.

When long-duration laser pulses pass through the column of plasma that may be formed from the working fluid, resonant de-excitation of the plasma may occur.

Simulations were performed using continuum mechanics, with the laser energy applied as a heat source in the working fluid, and also using radiation hydrodynamics, with the propagation and absorption of the laser beam simulated explicitly from the interface with the substrate. The computer programs used for these simulations were previously used to simulate the loading of samples tens of micrometers thick by laser ablation;<sup>13,14</sup> the numerical schemes were demonstrated to be accurate and consistent with each other.

#### A. Heat source simulations

Simulations were performed using one-dimensional continuum mechanics.<sup>15</sup> The axial profile of the flyer assembly was modeled, usually ignoring the Al and alumina layers as these had negligible mass compared with the substrate and the flyer, and it was observed from post-shot recovery that these materials were not vaporized by the laser drive. The power history of the laser pulse was deposited uniformly over the carbon layer, as a heating source term. An advantage of performing simulations with no explicit modeling of the absorption of laser energy or transport of thermal radiation is that material models and numerical representations of these behaviors can be ignored.

PMMA and Cu were modeled using empirical equations of state of the Grüneisen type.<sup>16</sup> Carbon (graphite) and Al were modeled using thermodynamically complete equations of state from the SESAME library,<sup>17</sup> necessary to allow heat deposition to be treated. The cell size was 20  $\mu\text{m}$  in the PMMA, 0.5  $\mu\text{m}$  in the carbon (one cell), and 5  $\mu\text{m}$  in the Cu.

Simulations were performed with the energy deposited over only part of the carbon layer, to assess the sensitivity to axial variations in heating. Simulations were also performed with the energy deposited uniformly over the carbon and an adjacent layer of Al 0.5  $\mu\text{m}$  thick. The acceleration history was fairly insensitive to these large changes in the working fluid. The acceleration was around 10% greater with the energy deposited over a smaller volume of carbon.

For uniform heating over the full thickness of the working fluid, peak drive pressures were predicted to lie in the range 0.4–1.1 GPa and peak temperatures from 12 000 to 44 000 K (1–4 eV). The acceleration histories exhibited the same qualitative trends as the experimental data, but the velocities were 10%–100% higher than observed, the highest discrepancies being for the thickest flyers. The temperature histories lay in three groups according to the laser energy (Figs. 8–10).

Given the predicted temperature history  $T(t)$ , heat loss by radiation through the substrate was estimated, assuming a blackbody. Taking representative peak temperatures for uniformly deposited heat and assuming radiative cooling over 2  $\mu\text{s}$ , the energy lost would be 0.05 J for 5 J laser energy (negligible), 0.5 J for 10 J laser energy (small), and 3–8 J for 20 J laser energy (significant). The greatest energy loss was for the highest laser energy and the thickest flyer: thicker flyers accelerate less quickly so the working fluid cools more

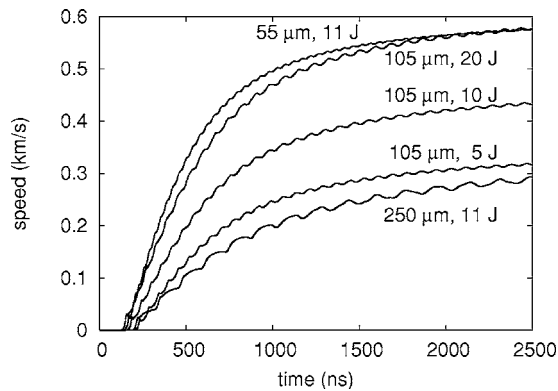


FIG. 8. Acceleration history, predicted with heat source applied uniformly over working fluid.

slowly by expansion; there is thus more opportunity for heat loss by radiation. These figures overpredict the radiated heat because the substrate is not transparent at all wavelengths and the working fluid is not a perfect blackbody, but it is likely that radiative cooling reduces the efficiency of acceleration at energies around 20 J or higher, particularly for flyers over 200 μm thick.

The simulations gave systematically higher predictions than the experimental data, the radiation hydrodynamic simulations falling higher than the heat source simulations. The shape of the predicted acceleration histories was broadly similar to the experimental records at early times, suggesting that loss of the working fluid through rupture of the confining layers was not an important effect during the early part of the acceleration. At later times for thicker flyers, the acceleration decreased more rapidly than in the predictions. This could be caused by rupture of the confining layers or by radial expansion with the layers intact.

## B. Laser deposition/radiation transport simulations

Simulations were performed using one-dimensional radiation hydrodynamics<sup>18</sup> to investigate the effect of physically realistic deposition profiles and energy transfer by thermal radiation. Radiation hydrocodes often do not treat transparent materials accurately, so the laser beam was treated as originating at the interface between the substrate and the carbon layer.

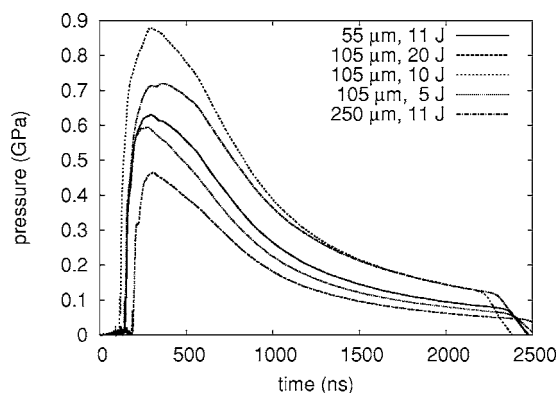


FIG. 9. Pressure history in working fluid, predicted with heat source applied uniformly over working fluid.

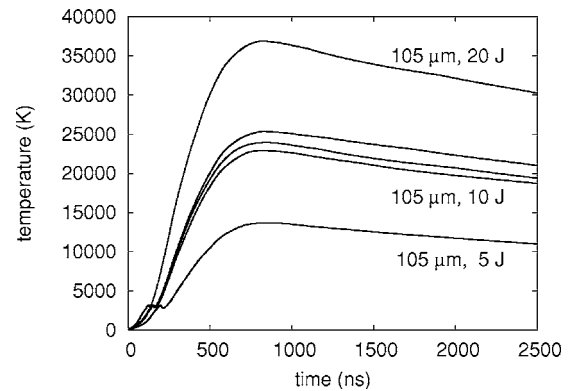


FIG. 10. Temperature history in working fluid, predicted with heat source applied uniformly over working fluid. (Central group from bottom to top: 105 μm, 10 J; 55 μm, 11 J; 250 μm, 11 J.)

These simulations are interesting in their own right. The laser irradiance and pulse length, and the confined plasma, explore regimes that are very unusual in laser-plasma terms. In fact, the irradiance in these experiments was two orders of magnitude smaller than the default numerical cutoff in the hydrocode below which laser deposition was ignored; the cutoff was reduced by a factor of  $10^4$  to allow the simulations to proceed.

Radiation hydrodynamics simulations are sensitive to the models used for absorption and emission of radiation, through the ionization model. Simulations were performed with Saha and Thomas-Fermi ionization; the results were not significantly different. Simulations were also performed with and without radiation transport (grey radiation diffusion) in the carbon; the acceleration histories were identical though the time taken to burn through the carbon was significantly different. Thomas-Fermi diffusion and grey radiation diffusion were used in subsequent simulations.

The radiation hydrodynamics simulations predicted similar pressure histories to the heat source simulations. Temperatures, though of the same magnitude as in the heat source simulations, were predicted to vary strongly with position through the working fluid. The acceleration histories exhibited the same qualitative trends as the experimental data and heat source simulations, but predicted velocities which were even greater than the heat source estimates.

It seems most likely that the radiation transport properties of carbon were not accurate enough to allow the radiation hydrodynamics simulations to improve over the heat source simulations, and in fact made them significantly less accurate. It was found when applying the heat source over only part of the carbon that the acceleration was slightly greater. The main difference between the heat source and laser deposition simulations is probably that the laser energy was mainly deposited close to the interface with the PMMA, which would lead to a more extreme partitioning of the energy. Since the heat source simulations reproduced the experimental data more faithfully, it seems likely that the heat was not redistributed fast enough in the laser deposition simulations. This could be caused by an opacity that was too high, or a thermal conductivity that was too low. The opacity was supplied in the form of SESAME tables, and the thermal

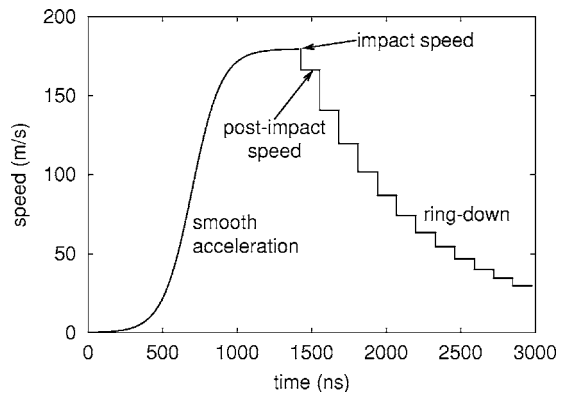


FIG. 11. Idealized velocity history for flyer acceleration and impact, based on 250  $\mu\text{m}$  flyer.

conductivity calculated from the ionization state. The discrepancy appeared after the initial acceleration, so the states in which thermal transport may be too low are carbon at temperatures of a few electron volts and mass densities of a few percent of the solid.

The accuracy of the radiation hydrodynamics simulations was encouraging enough to suggest that they could be the basis of a predictive capability including the effect of radiation transport properties. However, the simulations were not as accurate as the simpler heat source predictions when using the opacity and ionization models available, and thus are not recommended without further characterization of and improvements to these models.

## V. EQUATION OF STATE MEASUREMENTS FROM FLYER IMPACT

High pressure states were deduced from experiments in which the flyer impacted a transparent window. The deceleration on impact can be used to infer an unknown parameter on the principal shock Hugoniot of either the flyer or the window. If the EOS of the flyer and window are both known, the experiments can be used to investigate the accuracy of the technique.

### A. Impact-induced shock measurements

Ideally, the velocity history from the surface of the flyer should show a smooth acceleration to a well-established terminal speed, an abrupt deceleration on impact to a speed which remains constant for the time required for the shock wave to travel through the flyer and for a rarefaction to travel back, then a succession of decreasing decelerations as recompressions and rarefactions travel across the flyer (Fig. 11). Before impact, the velocity can be obtained directly from the Doppler shift. Afterwards, light reflects from the sample surface into the compressed window material, so the velocity should be calculated with respect to light traveling at the speed appropriate for the refractive index of the compressed material. The correction is negligible for PMMA.

Impact data for Cu flyers were obtained from five experiments (Table II). The VISAR records were used to determine the velocity history and flatness of each flyer. The impact of the flyer with the window was recorded, so we were able to measure the flatness directly after several hundred

TABLE II. Cu impact experiments.

| Shot   | Flyer                      |             | Postimpact speed<br>(m/s) |
|--------|----------------------------|-------------|---------------------------|
|        | Thickness( $\mu\text{m}$ ) | Speed (m/s) |                           |
| 14 139 | 250                        | 153 $\pm$ 2 | 150 $\pm$ 2               |
| 14 140 | 250                        | 180 $\pm$ 2 | 167 $\pm$ 2               |
| 14 147 | 55                         | 324 $\pm$ 1 | 297 $\pm$ 4               |
| 14 148 | 55                         | 573 $\pm$ 2 | 522 $\pm$ 2               |
| 14 149 | 55                         | 556 $\pm$ 2 | 503 $\pm$ 2               |

microns of flight. As discussed earlier, most of the flyers were still accelerating slightly at the end of the record. In most cases, after the initial deceleration on impact the velocity traces became more difficult to analyze, presumably because of damage causing changes to the optical properties of the window. There was some sign of ringing during acceleration, but no sign of shock formation or spall in the flyers (Fig. 12).

### B. Shock Hugoniot

The impact of the Cu flyer with the window provided a direct measurement of a point on the principal Hugoniot, with reference to the principal Hugoniot for the window. Reference Hugoniot were calculated from published EOS.<sup>16</sup> The Rankine-Hugoniot equations were solved numerically.<sup>19</sup>

The pressure regime explored was restricted to  $\sim 2$  GPa and less, because of the low shock impedance of the PMMA. This is desirable as a test that preheating of the flyer is low, as the effects may be obscured by higher-pressure impact states. Hugoniot points deduced from impact with the window were consistent with the published EOS for Cu. The laser flyer data followed the same trend as published data,<sup>20</sup> though the shock pressures were lower. Apart from the experiments at the lowest and highest pressures, the remaining points fell on the published Hugoniot to an accuracy an order of magnitude better than the estimated uncertainty, which was dominated by the uncertainty in particle speed. This suggests that the random errors may be less than the conservative estimates used here, but that there were sources of systematic error which did not manifest themselves in every experiment (Figs. 13 and 14).

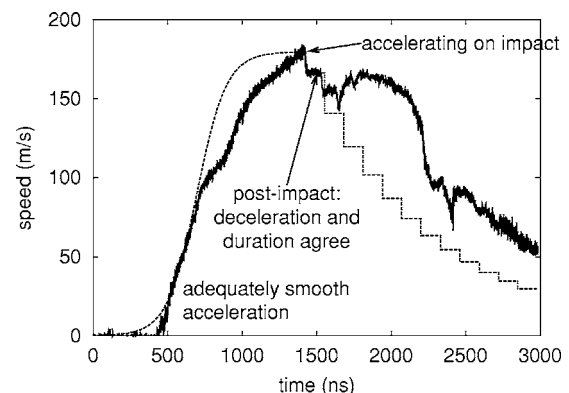


FIG. 12. Comparison between ideal velocity history and typical record (shot 14 140). The deviation between the records following the first reverberation after impact was caused by optical damage to the window.

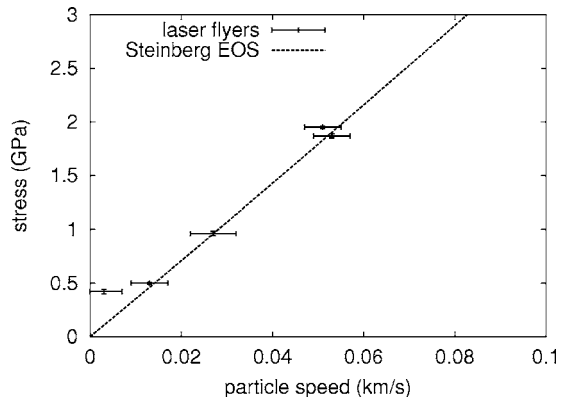


FIG. 13. Flyer Hugoniot points compared with Hugoniot from published equation of state. The Marsh points lying well below the curve are for porous samples.

The Hugoniot states would be sensitive to preheating in the flyer of around 500 K or greater. Any plausible preheating mechanism is likely to cause a significant temperature gradient through the flyer, which would be manifested as a velocity variation across the decelerated step in velocity following impact. From the flatness of the step, the preheat is estimated to be at most a factor of several smaller than 500 K.

## VI. DISCUSSION

The flyer acceleration experiments demonstrated that laser launching can be used for relatively thick flyers:  $\sim 50\text{--}250\ \mu\text{m}$  thick. The coated PMMA substrates performed reliably in this regime of laser irradiance ( $\sim 0.3\ \text{TW}/\text{m}^2$ ) and energy ( $\sim 0.2\ \text{MJ}/\text{m}^2$ ), and were inexpensive compared to alternatives such as sapphire. The irradiance and energy values are averages over the spot diameter: in principle, spatial variations—the speckle pattern—from a given laser and phase plate is likely to dictate the effective limit, and any given laser launch system (including substrate) should be expected to exhibit a catastrophic loss of efficiency as the energy is increased. The onset of this breakdown may be difficult to predict.

Comparing materials of different initial mass density and thickness, for a given laser energy, the velocity was similar for flyers of the same areal mass. The flyers were flat to within the accuracy of the velocity measurements, and

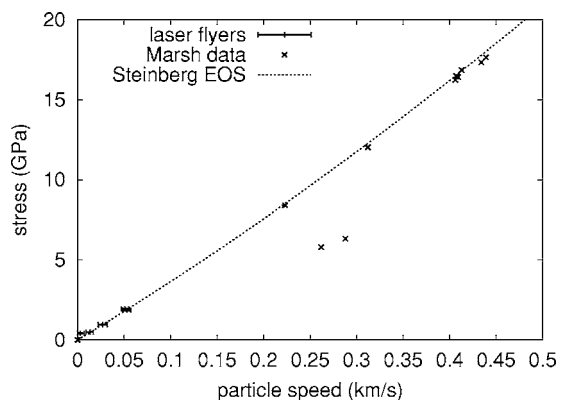


FIG. 14. Flyer Hugoniot points compared with published experimental data.

showed no sign of shock formation or spall, with the 600 ns drive pulse. These characteristics indicate that the laser-launching procedure is suitable for accurate shock physics experiments, and was demonstrated to operate in a regime of flyer thickness and speed which overlaps conditions accessible using proven gas gun techniques. In this range of thickness, the diameter of the flyer is still large enough to allow one-dimensional impact shock experiments to be performed.

Displacement histories deduced from the velocity history allowed the “barrel” length between the substrate and target to be constrained, to allow the flyer to reach its terminal speed. For the experiments considered here, the barrel length was in the range of a few hundred micrometers. The flyer travels a small fraction of its diameter before impact, so most of its diameter is free of edge effects.

The one-dimensional simulations of the flyer launch process reproduced systematic trends in the acceleration history with respect to variations in laser energy and flyer thickness. The simulations systematically overpredicted the speed reached by the flyers. Simulations in which the laser energy was deposited uniformly through the depth of the carbon working fluid were more accurate than simulations in which the laser deposition was calculated explicitly and heat transport was included by conduction and radiation. It seems likely that the opacity and heat conduction properties for carbon are inaccurate in the hot, expanded states explored in these experiments. It also seems likely that some laser energy was deposited in the PMMA substrates used, and that the drive plasma expanded or escaped laterally—particularly for thicker flyers. The level of agreement and capability for predicting systematic trends seems adequate to allow meaningful parameter studies to optimize the design of the flyer assembly, though considerable improvement in models of optical and transport properties of the substrate would be required before fully predictive simulations were possible. The simulations are also adequate to allow the performance of new systems to be predicted, assuming that the substrate is not close to breakdown.

The experimental Hugoniot points for Cu, deduced from the deceleration of the flyer on impact with a PMMA window, were generally in excellent agreement with the published equation of state. This consistency indicates that the flyers were not heated by the acceleration process to a degree where the shocked state was significantly affected, and certainly not to a level comparable with the working fluid or with a significant proportion of the laser energy appearing as heating of the flyer. The temperature of the working fluid—rather high in this case as its initial thickness was relatively small—can be misleading as its mass was low and there was little time for heat conduction to occur. Evidence from constant reflectivity of the flyer surface, the integrity of Ga flyers, and examination of recovered flyers indicates that any preheating was probably far below the level where it could affect shock measurements. The accuracy obtained in this particular case was  $\pm 5\ \text{m/s}$  and  $\pm 20\ \text{MPa}$ : certainly useful for shock physics studies.



## ACKNOWLEDGMENTS

Robert Hackenberg (MST-6) prepared and characterized the NiTi samples. The staff of TRIDENT contributed greatly to the conduct of the experiments. Jon Larsen (Cascade Applied Sciences, Inc.) gave advice on the use of the radiation hydrocode HYADES. The manuscript reviewers provided several useful suggestions to strengthen our inferences and conclusions. Funding for this work was provided by the Science and Technology Base Programs Office at Los Alamos National Laboratory (LANL), through Laboratory-Directed Research and Development (Directed Research) Project No. 2002-087, "New Windows into Shocks at the Mesoscale," Principal Investigator Aaron Koskelo (C-ADI). Support was also provided by the LANL Program Office for the National Nuclear Security Administration's Campaign 10, by the provision of time on the TRIDENT facility. The work was performed under the auspices of the U.S. Department of Energy under Contract No. W-7405-ENG-36.

<sup>1</sup>A. V. Bushman, G. I. Kanel', A. L. Ni, and V. E. Fortov, *Intense Dynamic Loading of Condensed Matter* (Taylor and Francis, London, 1993).

<sup>2</sup>D. L. Paisley, US Patent No. 5,029,528 (1991).

<sup>3</sup>D. L. Paisley, US Patent No. 5,046,423 (1991).

<sup>4</sup>D. B. Stahl and D. L. Paisley, US Patent No. 5,301,612 (1994).

<sup>5</sup>S. Watson and J. E. Field, *J. Appl. Phys.* **88**, 3859 (2000).

<sup>6</sup>S. Watson and J. E. Field, *J. Phys. D* **33**, 170 (2000).

<sup>7</sup>G. Zhuowei, S. Chengwei, Z. Jianheng, and Z. Ning, *J. Appl. Phys.* **96**, 344 (2004).

<sup>8</sup>K. Tanaka *et al.*, *Phys. Plasmas* **7**, 676 (2000).

<sup>9</sup>N. Ozaki *et al.*, *J. Appl. Phys.* **89**, 2571 (2001).

<sup>10</sup>K. Takamatsu *et al.*, *Phys. Rev. E* **67**, 056406 (2003).

<sup>11</sup>C. R. Phipps, J. P. Reilly, and J. W. Campbell, *Laser Part. Beams* **18**, 661 (2000).

<sup>12</sup>L. M. Barker and R. E. Hollenbach, *J. Appl. Phys.* **43**, 4669 (1972).

<sup>13</sup>D. C. Swift, T. E. Tierney IV, R. A. Kopp, and J. T. Gammel, *Phys. Rev. E* **69**, 036406 (2004).

<sup>14</sup>D. C. Swift, J. T. Gammel, and S. M. Clegg, *Phys. Rev. E* **69**, 056401 (2004).

<sup>15</sup>*Programs and Documentation for Hydrocode "LAGCID" V5.2* (Wessex Scientific and Technical Services, Perth, Scotland, 2001).

<sup>16</sup>D. J. Steinberg, Equation of state and strength properties of selected materials, Lawrence Livermore National Laboratory report UCRL-MA-106439 change 1 (1996).

<sup>17</sup>S. P. Lyon and J. D. Johnson (Los Alamos National Laboratory), SESAME: The Los Alamos National Laboratory equation of state database, Los Alamos National Laboratory report LA-UR-92-3407 (1992).

<sup>18</sup>*Programs and Documentation for Hydrocode "HYADES" V01.06.05* (Cascade Applied Sciences, Boulder, Colorado, 2004).

<sup>19</sup>"*ELECTRA*" *Software and Documentation* (Wessex Scientific and Technical Services, Perth, Scotland, 2000).

<sup>20</sup>*LASL Shock Hugoniot Data*, edited by S. P. Marsh (University of California, Berkeley, 1980).